Polarization analysis in resonant x-ray Bragg diffraction by K_2CrO_4 at the Cr K-edge

J. Fernández-Rodríguez,[1] S. W. Lovesey,[2,3] and J. A. Blanco[4]
[1]*European Synchrotron Radiation Facility, Boîte Postale 220, 38043 Grenoble Cedex, France*
[2]*ISIS Facility, Rutherford Appleton Laboratory, Oxfordshire OX11 0QX, United Kingdom*
[3]*Diamond Light Source Ltd., Oxfordshire OX11 0QX, United Kingdom*
[4]*Departamento de Física, Universidad de Oviedo, E-33007 Oviedo, Spain*
(Received 30 October 2007; revised manuscript received 11 February 2008; published 31 March 2008)

The creation of a circular polarization has been witnessed in resonant x-ray Bragg diffraction at the Cr K pre-edge (5.994 keV) of potassium chromate (K_2CrO_4). Interference between channels of diffraction and, specifically, the E1-E1, E2-E2, and E1-E2 channels provides an account of the observation. We report a theoretical analysis of polarization in the secondary beam for K_2CrO_4, with a variation of the primary linear polarization that successfully accounts for all aspects of the observations. An angular anisotropy of the local environment at Cr sites in this material is revealed in time-even quadrupoles, octupoles, and hexadecapoles that appear in scattering amplitudes for parity-even (E1-E1 and E2-E2) and parity-odd polar (E1-E2) channels. Our estimates of the multipoles derived from a fitting to the data for the secondary polarization are exploited in simulations of the diffracted intensity as a function of the azimuthal angle. There is a satisfactory agreement between simulations and the total intensity measured at space-group-forbidden (140) and (340) reflections.

DOI: 10.1103/PhysRevB.77.094441 PACS number(s): 78.70.Ck, 78.20.Bh, 78.20.Ek

I. INTRODUCTION

The charge, orbital, and spin degrees of freedom of the few electrons in the valence states of a material are central to its electronic properties. Dominant today among the experimental techniques that measure these microscopic variables is resonant x-ray scattering (RXS), which is enhanced by the brightness, tunability, and high degree of polarization enjoyed at x-ray synchrotron sources. In this technique, by studying intensities at space-group-forbidden reflections, different multipolar order parameters can be studied: magnetic dipoles, quadrupoles, octupoles, anapoles, etc. Only recently has it become possible to access such ordering phenomena by means of resonant x-ray diffraction.[2–7]

One paradigmatic complex material that has attracted attention during the past decade is potassium chromate[8,9] (K_2CrO_4). RXS experiments at resonances 13 eV below the Cr K-edge show large changes in intensity with the rotation of the crystal about the Bragg wave vector (an azimuthal angle scan) for weak forbidden Bragg reflections.[8] Recently, in a crucial experiment in K_2CrO_4 by Mazzoli *et al.*[10] carried out at beamline ID20 (Ref. 11) of the ESRF, after a very considerable detailed technical and engineering effort invested by this research group, they illustrated quite well how to address well-known problems in RXS (such as the existence of twinning or mosaicity in the samples, the absorption corrections for nonspecular reflections, and the most difficult one, which is the need to be sure that one illuminates the same single crystal when the sample is rotated about the scattering vector during an azimuthal scan) by extending the well-known techniques of optical polarimetry to the x rays. The experiment of Mazzoli *et al.* clearly shows that measuring the Stokes parameters of the secondary beam as a function of the primary one could be quite useful in explaining the effects of interference between dipole and quadrupole (or other types, in general) transitions, leading to phase shifts between the respective scattering amplitudes. In this way, the x-ray polarization analysis can also be used to separate the contributions of two resonances, which are quite close in energy (about 1 or 2 eV) and thus appear as a single pseudopeak in an energy scan.

In their experiment Mazzoli *et al.*[10] performed RXS measurements on the space-group-forbidden reflection (130) of K_2CrO_4. Additionally, they used a diamond phase plate crystal, which allows continuous change in the polarization of the primary x-ray beam. By using this setup, Stokes parameters were determined by fitting the dependence of the secondary intensity with the angle of rotation of the polarization analyzer. Perhaps most interestingly, Mazzoli *et al.* reported the creation of circular polarization in a resonant Bragg diffraction, which they attributed to coherent interference.

We report a complete theoretical analysis of RXS at the Cr K-edge that demonstrates circular x-ray polarization created at the Cr pre-edge (5.994 keV) through the interference of amplitudes from resonant events. The interference leads to a phase shift between the respective scattering amplitudes in different polarization channels. Our work is based on exact expressions for parity-even and parity-odd resonant amplitudes of scattering.[1] These amplitudes are evaluated with an atomic model of valence electron states that complies with the established crystal structure of potassium chromate. In our report, we include predictions for an azimuthal angle scan and a fit to the available data.

K_2CrO_4 is nonmagnetic, and it crystallizes in the orthorhombic space group *Pnma* (number 62), which is centrosymmetric (crystal class D_{2h}). Cr ions are located in the Wyckoff positions 4*c* on the mirror plane, which is at the center of a nearly regular oxygen tetrahedron. Reflections (*hk*0) with integer Miller indices and odd *h* are blocked by a glide plane in $(x,y,1/4)$.

II. CALCULATION OF THE RESONANT AMPLITUDES

The scattering amplitude, in units of the classical radius of the electron, is represented in terms of four components $G_{\mu\nu}$,

where μ and ν denote states of polarization that are labeled σ or π. Expressions in terms of $G_{\mu\nu}$ for the intensity I_0 and secondary Stokes parameters P_1', P_2', and P_3' are given in Appendix A.

The absorption spectrum as a function of x-ray energy $E=\hbar cq$, which was reported by Mazzoli *et al.*,[10] contains a sharp feature without any appreciable structure at 5.994 keV, which is well below the principal contribution to absorption. It is reasonable to represent such an energy feature by a single oscillator. Thus, we express a component of the scattering amplitude as $G=d(E)Z$, where $d(E)$ is an energy denominator,

$$d(E) = \frac{\Delta}{E - \Delta + i\Gamma/2}, \tag{1}$$

where Δ is the energy and Γ is the width of the resonance. Here, the polarization dependence of Γ is solely in the amplitude factors Z. These are written in terms of dimensionless unit-cell structure factors F [1]

$$Z(\text{E1-E1}) = \left(\frac{\{R\}_{sp}}{a_0}\right)^2 \left(\frac{m\Delta a_0^2}{\hbar^2}\right) F(\text{E1-E1}), \tag{2}$$

$$Z(\text{E2-E2}) = \left(\frac{q\{R^2\}_{sd}}{a_0}\right)^2 \left(\frac{m\Delta a_0^2}{\hbar^2}\right) F(\text{E2-E2}), \tag{3}$$

$$Z(\text{E1-E2}) = \left(\frac{q\{R^2\}_{sd}\{R\}_{sp}}{a_0^2}\right) \left(\frac{m\Delta a_0^2}{\hbar^2}\right) F(\text{E1-E2}), \tag{4}$$

where a_0 is the Bohr radius and $\{R\}_{sp}$ is a radial integral for the s-p absorption event. The generic form of a unit-cell structure factor is

$$F = \sum_K \boldsymbol{J}^K \cdot \boldsymbol{D}^K \cdot \boldsymbol{\Psi}^K. \tag{5}$$

The three spherical tensors of rank K are as follows: $\boldsymbol{J}^K$ describes properties of the x-ray beam, $\boldsymbol{D}^K$ is a rotation that establishes the setting of the crystal with respect to axes that define the plane of scattering and states of polarization, and $\boldsymbol{\Psi}^K$ is a structure factor for electron states in a unit cell of the crystal that accept electrons photoejected from a $1s$ core state. The values of $\boldsymbol{J}^K$ that are appropriate for E1-E1, E2-E2, and E1-E2 events are denoted here by $\boldsymbol{X}^K$, $\boldsymbol{H}^K$, and $\boldsymbol{N}^K$, and the components are listed in Ref. 1.

We use Cartesian coordinates (xyz) for the geometry of the scattering experiment.[1] The plane of scattering is spanned by the x-y axes, with the Bragg wave vector $\boldsymbol{\tau}(hkl)$ in the opposite direction to the x axis, and σ polarization parallel to the z axis. In the experiment performed on K_2CrO_4,[10] the c axis is initially parallel to the z axis. With this setting of the crystal, the operation $\boldsymbol{D}^K$ makes $\boldsymbol{\tau}$ parallel to $-x$ by a rotation through an angle α about the z axis. For an $(hk0)$ reflection, α is given by $\tan\alpha = -(\boldsymbol{\tau}_b/\boldsymbol{\tau}_a) = -(ak/bh)$, where $\boldsymbol{\tau}_a$ and $\boldsymbol{\tau}_b$ are components of the Bragg wave vector $\boldsymbol{\tau}(hkl)$, the cell lengths are $a=7.662$ Å, $b=5.919$ Å, and $c=10.391$ Å,[8] and $\alpha=104.4°$ at the (130) reflection.

In an atomic model, $\boldsymbol{\Psi}^K$ is expressed in terms of atomic multipoles that are expectation values, or time averages, of spherical tensor operators. We denote the expectation value by angular brackets around the operator. An expectation value is calculated with a valence state that accepts the photoejected electron in a specified absorption event. Thus, a multipole is an equilibrium property of the ground state of the compound. Multipoles that describe parity-even events are not changed by the inversion operation. On the other hand, in a parity-odd event, the multipoles change sign when acted on by the inversion operator.[1] With parity-even multipoles, there is a one to one correspondence between the multipole's rank K and the behavior of the multipole with respect to the reversal of time, namely, even (odd) rank multipoles are time even (odd). Since K_2CrO_4 does not support a spontaneous magnetic order and no magnetic field is applied to the sample, we only need to consider time-even multipoles here. The time-even multipoles in a parity-odd event are usually called polar multipoles.

Let us construct the structure factors $\boldsymbol{\Psi}^K$. K_2CrO_4 crystallizes in a structure where the four resonant Cr ions at sites $4c$ have positions in crystallographic coordinates given by $\mathbf{d}_1=(x,1/4,z)$, $\mathbf{d}_2=(1/2-x,3/4,1/2+z)$, $\mathbf{d}_3=(-x,3/4,-z)$, and $\mathbf{d}_4=(1/2+x,1/4,1/2-z)$. The environments of ions 1 and 3 and ions 2 and 4 are related by a spatial inversion I, while the environments at sites 1 and 4 are related by a mirror plane normal to the z axis and represented by $m_z=IC_{2z}$, where C_{2z} is the rotation by π about the z axis. The site symmetry is m_y, and with this element of symmetry, the operator C_{2z} relates to environments 1 and 2.

For an arbitrary spherical tensor of rank K and projection $Q(-K\leq Q\leq K)$, the operation C_{2z} is equivalent to a phase factor $(-1)^Q$. The quantity Ψ_Q^K for parity-even events and reflections of the kind $(hk0)$ is found to be

$$\Psi_Q^K = \sum_{\boldsymbol{d}} \exp(i\boldsymbol{d}\cdot\boldsymbol{\tau})\langle T_Q^K\rangle = 2\cos(\varphi+\pi k/2)\langle T_Q^K\rangle[1+(-1)^{h+Q}], \tag{6}$$

where $\varphi=2\pi hx$, with $x=0.2291$, and $\langle T_Q^K\rangle$ is a multipole for parity-even events (E1-E1 and E2-E2). In Eq. (6), there is a selection rule constraining $h+Q$ to be an even integer. Space-group-allowed reflections are such that the diagonal element Ψ_0^K is different from zero. Reflections $(hk0)$ with odd h are space group forbidden since $\Psi_0^K=0$.

Parity-odd and time-even tensors are denoted by $\langle U_Q^K\rangle$. The corresponding structure factor is

$$\Psi_Q^{K,u} = 2i\sin(\varphi+\pi k/2)\langle U_Q^K\rangle[1-(-1)^{h+Q}], \tag{7}$$

and diffraction can occur for odd $h+Q$. As expected for a centrosymmetric crystal structure, expression (7) vanishes in the forward direction of scattering (zero deflection), for which the Miller indices $h=k=l=0$. As a consequence, potassium chromate does not display a natural circular dichroism.[1]

All of our atomic multipoles, $\langle T_Q^K\rangle$ and $\langle U_Q^K\rangle$, satisfy the relation $\langle T_Q^K\rangle^* = (-1)^Q\langle T_{-Q}^K\rangle$, where * denotes a complex conjugation. The point symmetry m_y requires $\langle T_Q^K\rangle = (-1)^K I\langle T_Q^K\rangle^*$, which follows from the use of the identity $C_{2y}\langle T_Q^K\rangle = (-1)^{K+Q}\langle T_{-Q}^K\rangle$. Thus, for even K (odd K), multi-

poles are purely real (imaginary) for parity-even (odd) events. With even K, one has $\langle U_0^K\rangle = -\langle U_0^K\rangle$ and, thus, $\langle U_0^K\rangle = 0$.

Henceforth, we take the Miller index h to be an odd integer and establish the properties of the corresponding structure factors [Eqs. (6) and (7)]. Parity-even events have even K because the material has no magnetic structure, while Eq. (6) can be different from zero when the projection Q is an odd integer. For this case, Ψ_Q^K is purely real, and $\Psi_{-Q}^K = -\Psi_Q^K$; i.e., Ψ_Q^K is an odd function of Q. The E1-E1 amplitude contains quadrupoles ($K=2$), and the E2-E2 amplitude is a linear combination of quadrupoles and hexadecapoles ($K=4$).

The parity-odd E1-E2 amplitude is a sum of multipoles with ranks $K=1$, 2, and 3, and $K=3$ is an octupole. In a parity-odd amplitude, quadrupoles are pseudotensors, while dipoles and octupoles are true tensors. Since h is odd, the projection Q is an even integer. In this case, we find $\Psi_{-Q}^{K,u} = -\Psi_Q^{K,u}$ for even K and for odd K $\Psi_{-Q}^{K,u} = \Psi_Q^{K,u}$.

Expressions for the unit-cell structure factors $F_{\mu\nu}$(E1-E1), $F_{\mu\nu}$(E2-E2), and $F_{\mu\nu}$(E1-E2) are given in Appendix B. These expressions are valid for a rotation by ψ about the Bragg wave vector $\boldsymbol{\tau}$ away from the setting $\psi=0$, at which the crystal c axis is normal to the plane of scattering.

III. CALCULATION OF SECONDARY STOKES PARAMETERS

The intensity of a diffracted peak for states of primary polarization described by Stokes parameters $\boldsymbol{P}=(P_1,P_2,P_3)$ and expressed in terms of $G_{\mu\nu}$ is found in Appendix A. (Note that the notation for the Stokes parameters used in this work is that of Refs. 12 and 13, and our parameters P_1, P_2, and P_3 correspond to P_2, P_3, and P_1, respectively, in the work of Mazzoli *et al.*[10]) When the primary polarization is linear, the mean helicity in the primary beam is zero and $P_2=0$. The primary linear polarization subtends an angle η with the z axis, which is parallel to the σ component of polarization. The Stokes parameters are then $P_1=\sin(2\eta)$, $P_2=0$, and $P_3=\cos(2\eta)$, relating $\eta=0$ to σ polarization. In the work by Mazzoli *et al.*,[10] an estimation of the square of the secondary beam circular polarization is obtained from $(P_2')^2=1-(P_1')^2-(P_3')^2$, which is only valid in the case of a completely polarized beam.

By way of an orientation to our full analysis of the data for secondary polarization, which was reported by Mazzoli *et al.*,[10] we begin with a calculation of P_2' when the crystal c axis is normal to the plane of scattering. This setting of the crystal corresponds to $\psi=0$, and an inspection of results in Appendix B shows that all structure factors for unrotated channels of polarization are zero. This result can be traced to the selection rules on Q noted above, the properties of $\boldsymbol{X}^K$, $\boldsymbol{H}^K$, and $\boldsymbol{N}^K$,[1] and the fact that for $\psi=0$ in Eq. (5), the rotation matrix $D_Q^K=\exp(iQ\alpha)$ for all K.

With $F_{\sigma'\sigma}=F_{\pi'\pi}=0$ for all resonance channels, we find from Eq. (A3) that P_2' is proportional to P_1, namely, $P_2' \propto -P_1\,\mathrm{Im}(G^*_{\pi'\sigma}G_{\sigma'\pi})$. Using a single resonance model, with the resonance energy in $d(E)$ set at $\Delta=5.994$ keV, means that $G_{\mu\nu} \propto d(E)F_{\mu\nu}$, and for this model, $\mathrm{Im}(G^*_{\pi'\sigma}G_{\sigma'\pi})=0$ because all the unit-cell structure factors $F_{\mu\nu}$ are purely real.

A value of P_2' other than zero is possible when $G_{\mu\nu}$ is taken to be a coherent sum of resonant contributions at different energies, i.e., Δ_1 and Δ_2. By denoting the corresponding resonant energy denominators by $d_1(E)$ and $d_2(E)$, we may take $G_{\sigma'\pi}=Z_1(\sigma'\pi)d_1(E)+Z_2(\sigma'\pi)d_2(E)$, where $Z_1(\sigma'\pi)$ and $Z_2(\sigma'\pi)$ are purely real. For this model,

$$\mathrm{Im}(G^*_{\pi'\sigma}G_{\sigma'\pi}) = [Z_2(\pi'\sigma)Z_1(\sigma'\pi) - Z_2(\sigma'\pi)Z_1(\pi'\sigma)]\mathrm{Im}\{d_2(E)^*d_1(E)\}.$$

After inserting unit-cell structure factors, the quantities to be determined from the experimental data are the various atomic multipoles.

The result for P_2' at $\psi=0$ discussed in the previous paragraph has a shortcoming, and so do the corresponding results for other Stokes parameters of the secondary beam. This prevents a successful analysis of the experimental data if we use $\psi=0$. The shortcoming is seen in the variation of calculated secondary Stokes parameters as a function of the angle η. Calculated Stokes parameters are symmetric (P_3') or antisymmetric (P_1' and P_2') about $\eta=0$. These symmetries are not found in the data provided in Fig. 5 of Mazzoli *et al.*[10] A fitting of the Stokes parameter data to a model with $\psi=0$ cannot account for the experimental variations. We have concluded that it is important to take into account the fact that in their experiment, Mazzoli *et al.* did not have the crystal aligned with the c axis normal to the plane of scattering, and the azimuthal angle ψ is actually different from zero. We therefore turn to an analysis of the data by using expressions from Appendix B with $\psi \neq 0$, for which all unit-cell structure factors $F_{\mu\nu}$ can be different from zero.

In our analysis of the experimental data, we are led to consider a model with single oscillator amplitudes for the E1-E1, E2-E2, and E1-E2 event resonances centered at different energies Δ_i with different widths Γ_i. The total amplitude G is now taken to be

$$\begin{aligned} G &= G(\text{E1-E1}) + G(\text{E2-E2}) + G(\text{E1-E2}) \\ &= \rho_{\text{E1-E1}}F(\text{E1-E1}) + \rho_{\text{E2-E2}}F(\text{E2-E2}) + \rho_{\text{E1-E2}}F(\text{E1-E2}). \end{aligned} \tag{8}$$

Here, E is the energy of the incident x-rays (5.994 keV). ρ_i are complex numbers given by the resonant denominators in Eq. (1). In the fitting, the modulus of Eq. (1) and the factors in Eqs. (2)–(4) are considered included in the fitting values of the atomic tensors $\langle T_Q^K\rangle$ and $\langle U_Q^K\rangle$ in Eqs. (B1)–(B9) as they only represent multiplicative constants.

IV. FITTING OF THE MODEL TO THE EXPERIMENTAL DATA

We fit the dependence of the Stokes parameters of the secondary beam with the angle η of the linear primary polarization together with the secondary Stokes parameters determined for the primary circular polarization $P_3'=-0.383$ and $P_1'=-0.522$ (Ref. 10) for the (130) reflection. The calculations have used the nonzero azimuthal angle $\psi=-0.783°$

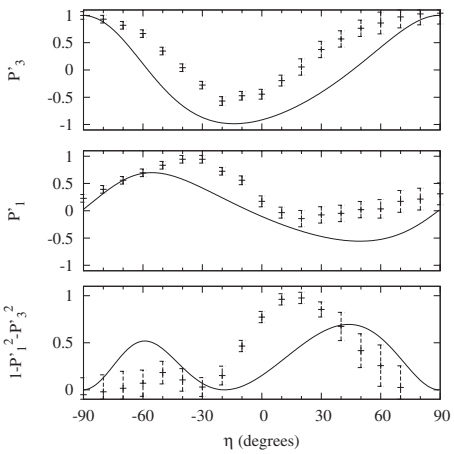

FIG. 1. Fit of the dependence of the Stokes parameters of the secondary beam with the angle η of the linear primary polarization in the case of contributions from the E1-E1 and E1-E2 channels for the (130) reflection. It is assumed that there is no E2-E2 contribution. The azimuthal angle used is $\psi=-0.783°$, as reported in Ref. 10 The fitted parameters are shown in Eq. (9). Together with the data plotted in the figure, for primary circularly polarized light with $P_2=+1$, the fitting gives secondary Stokes parameters $P_3'=-0.338$ and $P_1'=-0.865$ (in agreement with the experimental values (Ref. 10) $P_3'=-0.383$ and $P_1'=-0.852$).

reported by Mazzoli *et al.*[10] We consider a general model with contributions from the parity-even E1-E1 and E2-E2 channels and the parity-breaking E1-E2 channel. We account for the positioning in energy of the resonances by the phases of the factors ρ_i in Eq. (8). It is important to note that it is not possible to infer the exact position in energy Δ of each resonance because two undetermined quantities, i.e., Γ and Δ, appear in the Lorentzian denominator. In order to reduce the

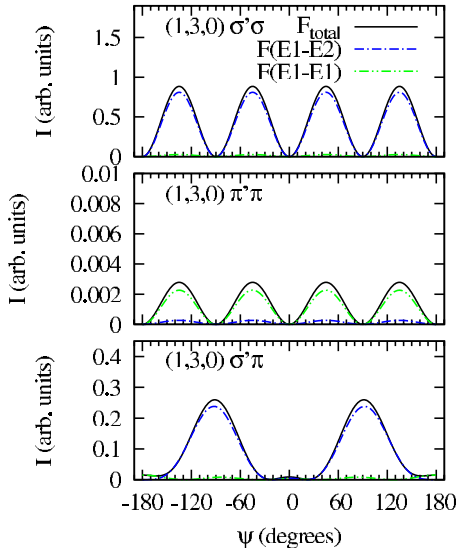

FIG. 2. (Color online) Azimuthal dependence of the intensity of the (130) reflection derived from the model with contributions only from E1-E1 and E1-E2 channels (the total intensity and derived intensities from each of the resonant events are shown). To obtain these curves, the fitted parameters in Eq. (9) were used.

fitting parameters and eliminate the dependence on a global phase and a global amplitude, we have used $\rho_{\text{E1-E1}}=i$ and $\text{Re}\langle T_1^{2,\text{E1-E1}}\rangle=1$.

The first attempt to fit data has been made considering the fact that multipoles derived from the E2-E2 resonant event are expected to be zero in an atomic localized approximation because the chromium ion is Cr^{6+} $(3d^0)$ in K_2CrO_4 and the empty $3d$ shell is spherically symmetric. On account of this, we attempt a fitting in which the F(E2-E2) is assumed to be zero, and only E1-E1 and E1-E2 resonances are present. The result is shown in Fig. 1, and the fitting parameters are shown below:

$$\text{Re}\ \rho_{\text{E1-E2}} = 45.3 \pm 0.7,$$

$$\text{Im}\ \rho_{\text{E1-E2}} = 7.5 \pm 0.7,$$

$$\text{Re}\langle U_0^1\rangle = 15.073 \pm 0.004$$

$$\text{Re}\langle U_0^3\rangle = 3.553 \pm 0.005,$$

$$\text{Im}\langle U_2^2\rangle = -2.513 \pm 0.003,$$

$$\text{Re}\langle U_2^3\rangle = 5.966 \pm 0.003. \quad (9)$$

Although the fitted curves follow the tendency of the data, the agreement with experimental data in Fig. 1 is not totally satisfactory. The azimuthal dependence of the intensity calculated from the parameters in Eq. (9) for the (130) reflection is plotted in Fig. 2. The intensities derived from E1-E1 and E1-E2 resonances are shown. The result that we obtain shows that when considering the azimuthal dependence, the intensity is mainly produced by the parity-breaking E1-E2 event, and only the parity-even E1-E1 event has a strong influence in the weak signal that would appear in the $\pi'\pi$ channel.

We also plot the results that would be obtained for the azimuthal dependence of the (140) and (340) reflections with the set of parameters we have fitted in Fig. 3. In the plots, we have assumed that at $\psi=0$, the c axis is initially parallel to the z axis in the x-ray coordinates.[1] The angles α calculated for these reflections are $\alpha_{(140)}=100.9°$ and $\alpha_{(340)}=120.1°$. The primary linear polarization used is σ, and it is assumed that no polarizer is used for measuring the intensity of the secondary beam. Thus, the total intensity displayed in Fig. 3 is I_0 in Eq. (A1) evaluated with $P_1=P_2=0$ and $P_3=+1$. It can be noted that in the plot, for the (140) and (340) reflections, the E1-E2 event intensity is strongly enhanced with respect to the E2-E2 parity-even amplitude due to the value of φ for the (140) reflection, i.e., $\varphi=2\pi hx=1.44$, which is close to $\pi/2$, and in the case of (340) $\varphi=4.32$, which is close to $3\pi/2$. According to Eq. (6), these values of φ will lead to a negligible E2-E2 contribution, which is almost zero for these two Bragg reflections. Azimuthal angle measurements for (140) and (340) reflections have been published in Ref. 8 (note that they use a different convention for the origin of the azimuthal angle). In these plots, the (140) and (340) reflections would be more intense than the (130) one with an enhancement of the maximum intensities by about 2 orders of

magnitude. The shape of the azimuthal curves does not agree with the curves published in Ref. 8.

The second attempt for fitting the experimental variations includes E2-E2 resonant events. The best fit to the experimental data (Fig. 4) leads to the following parameters:

$$\text{Re}\ \rho_{\text{E2-E2}} = -3.31 \pm 0.07,$$

$$\text{Im}\ \rho_{\text{E2-E2}} = -8.12 \pm 0.03,$$

$$\text{Re}\ \rho_{\text{E1-E2}} = 23.3 \pm 0.2$$

$$\text{Im}\ \rho_{\text{E1-E2}} = 19.37 \pm 0.10,$$

$$\text{Re}\langle T_1^{2,\text{E2-E2}}\rangle = -24.08 \pm 0.06,$$

$$\text{Re}\langle T_1^{4,\text{E2-E2}}\rangle = 103.7 \pm 0.2,$$

$$\text{Re}\langle T_3^{4,\text{E2-E2}}\rangle = 6.44 \pm 0.16,$$

$$\text{Re}\langle U_0^1\rangle = 13.7 \pm 0.4,$$

$$\text{Re}\langle U_0^3\rangle = -28.2 \pm 0.5,$$

$$\text{Im}\langle U_2^2\rangle = -52.2 \pm 0.2,$$

$$\text{Re}\langle U_2^3\rangle = -51.9 \pm 0.3. \quad (10)$$

In Fig. 4, the fitted curves describe the experimental data with excellent agreement. The predicted shape of the azimuthal dependence of the (130) reflection for this set of parameters is shown in Fig. 5, and those of the (140) and (340) reflections are shown in Fig. 6, showing the total contribution of the different resonances to the intensity. The E2-E2 event is the dominant contribution to the intensity over the amplitudes produced by the other resonances for the (130) reflection, but in the case of (140) and (340) reflections the E2-E2 contribution is almost zero because of the particular value of $(\varphi+\pi k/2)$ for those reflections. The order of magnitude for the maximum intensities in the azimuthal dependence of (130), (140), and (340) reflections is approximately the same. The shape of the azimuthal dependence of (140) and (340) reflections presents a better qualitative agreement with the data in Ref. 8 compared to that in the model without E2-E2, as previously discussed. However, the presence of the E2-E2 contribution seems to clash with the prediction of a small value for E2-E2 atomic tensors due to the spherical symmetry of the Cr^{6+} $3d^0$ shell for the isolated Cr ion. This result seems to indicate that the Cr^{6+} ions have an electron density that is not spherically distributed around the nucleus owing to strong covalency with the neighboring oxygen ions.[9] This prediction deserves additional checking of experimental work.

Also, a fit of the dependence of the Stokes parameters by using a model with intensities coming only from parity-even events (E1-E1 and E2-E2) has been made in an attempt to use a model similar to that of Mazzoli *et al.*[10] Although the number of fitting parameters is reduced we continue to choose $\rho_{\text{E1-E1}}=i$ and $\text{Re}\langle T_1^{2,\text{E1-E1}}\rangle=1$. The parameters obtained in the fit are

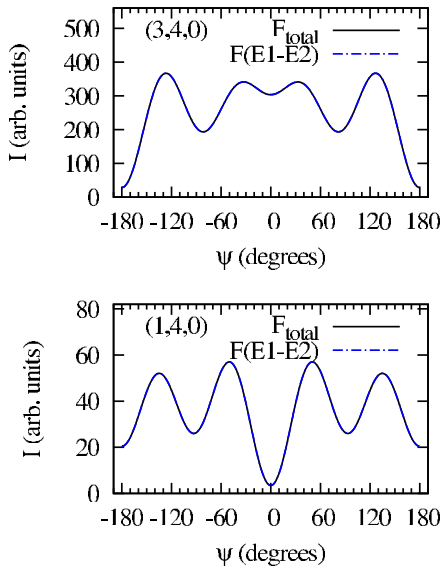

FIG. 3. (Color online) Azimuthal dependence of the intensity of the (140) and (340) reflections derived from the fitted parameters in Eq. (9). The total intensity I_0 in Eq. (A1) and the derived intensities from the E1-E2 event are shown. The contribution from the E1-E1 channel is negligible. The primary linear polarization used is σ, and it is assumed that no polarizer is used for measuring the intensity of the secondary beam. We assume that at $\psi=0$, the c axis is initially parallel to the z axis in the x-ray coordinates (Ref. 1).

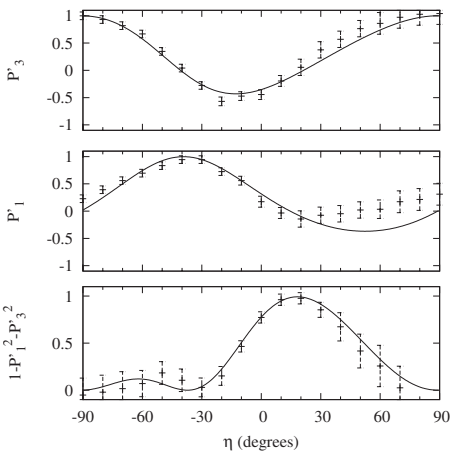

FIG. 4. Fit of the dependence of the Stokes parameters of the secondary beam with the angle η of the linear primary polarization in the case of contributions from a Lorentzian for each of the resonant events E1-E1, E2-E2, and E1-E2 when considering the azimuthal angle $\psi=-0.783°$ reported in Ref. 10 for the (130) reflection. Fitted parameters are shown in Eq. (10). Together with the data plotted in the figure, for primary circularly polarized light with $P_2=+1$, the fitting gives secondary Stokes parameters $P_3'=-0.381$ and $P_1'=-0.854$ (in agreement with the experimental values $P_3'=-0.383$ and $P_1'=-0.852$).

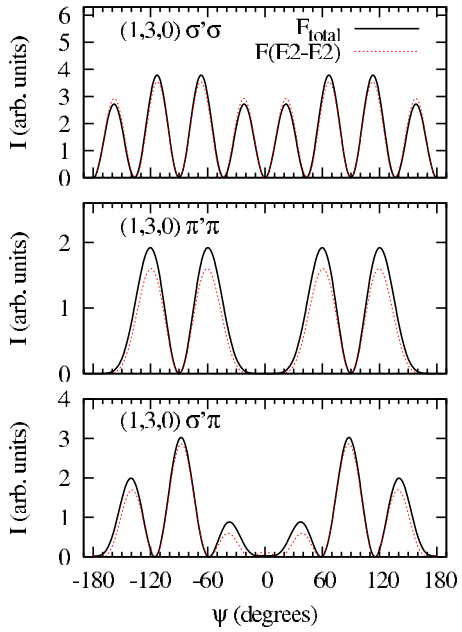

FIG. 5. (Color online) Azimuthal dependence of the intensity of the (130) reflection derived from the model contributions from all parity-even and parity-odd channels (the total intensity and derived intensities from each of the resonant events are shown). E1-E1 and E1-E2 intensities are not shown because they are negligible. To obtain these curves, the fitted parameters in Eq. (10) were used.

$$\text{Re}\ \rho_{\text{E2-E2}} = -0.082 \pm 0.001,$$

$$\text{Im}\ \rho_{\text{E2-E2}} = 0.542 \pm 0.001,$$

$$\text{Re}\langle T_1^{2,\text{E2-E2}}\rangle = -1.530 \pm 0.004,$$

$$\text{Re}\langle T_1^{4,\text{E2-E2}}\rangle = 9.83 \pm 0.01,$$

$$\text{Re}\langle T_3^{4,\text{E2-E2}}\rangle = -1.52 \pm 0.01. \quad (11)$$

Figure 7 shows an agreement with the experimental data that is not completely satisfactory. In Figs. 8 and 9, we plot the azimuthal variations of (130), (140), and (340) reflections. The shapes of (140) and (340) do not agree with the data published in Ref. 8, and the intensity in those reflections would be much weaker than (130) as the factor $\cos(\varphi+\pi k/2)$ in Eq. (6) is reduced for (140) and (340) reflections. All this leads us to discard this model.

It appears from the present work that it is highly necessary in resonant x-ray diffraction experiments to combine information obtained from both azimuthal angle scans and polarization analysis at some selected azimuthal angles. Due to the number of characteristic features to be described, fitting the results of only one of those two types of experiments does not lead to a unique set of physical meaningful parameters. On the other hand, cross-checks between these two types of measurements are necessary in determining a common solution.

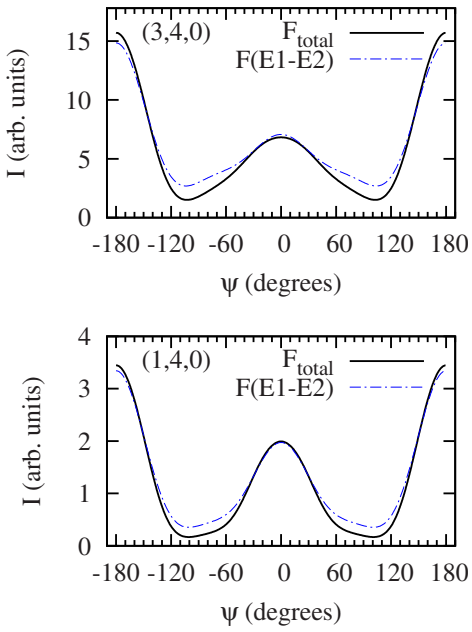

FIG. 6. (Color online) Azimuthal dependence of the intensity of the (140) and (340) reflections derived from the fitted parameters of the model with contributions from the E2-E2 and E1-E2 channels. E1-E1 and E2-E2 intensities are not shown because they are negligible. To obtain these curves, the fitted parameters in Eq. (10) were used. The primary linear polarization used is σ, and it is assumed that no polarizer is used for measuring the intensity of the secondary beam. We assume that at $\psi=0$, the c axis is initially parallel to the z axis in the x-ray coordinates (Ref. 1).

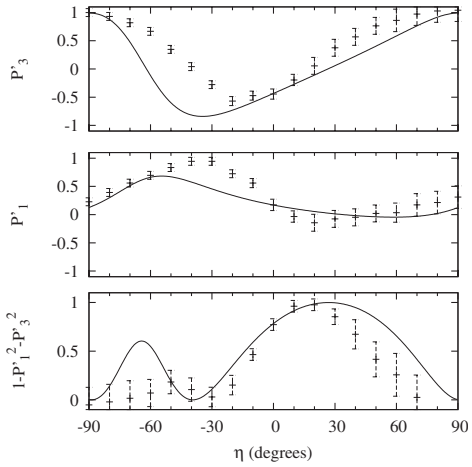

FIG. 7. Fit of the dependence of the Stokes parameters of the secondary beam with the angle η of the linear primary polarization in the case of contributions from the E1-E1 and E2-E2 channels. It is assumed that there is no E1-E2 contribution. The azimuthal angle used is $\psi=-0.783°$, as reported in Ref. 10. Fitted parameters are shown in Eq. (11). Together with the data plotted in the figure, the secondary Stokes parameters $P_3'=-0.368$ and $P_1'=-0.840$ obtained for primary circularly polarized light with $P_2=+1$ (agreeing with the experimental values $P_3'=-0.383$ and $P_1'=-0.852$) have been considered in the fitting.

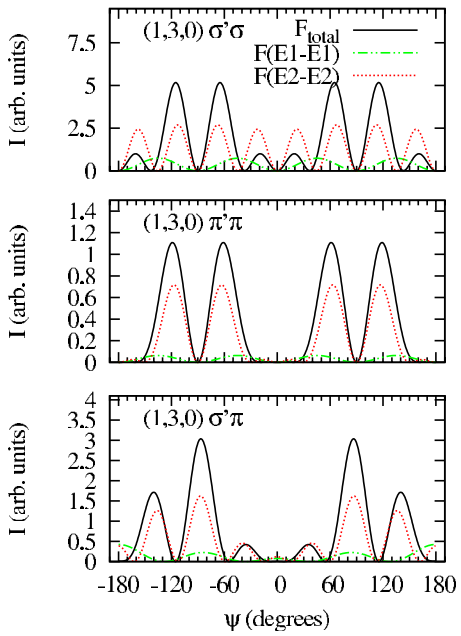

FIG. 8. (Color online) Azimuthal dependence of the intensity of the (130) reflection derived from the model contributions from all parity-even and parity-odd channels (the total intensity and derived intensities from each of the resonant events are shown). To obtain these curves, the fitted parameters in Eq. (11) were used.

V. CONCLUSIONS

We have performed a theoretical analysis of experimental data, which were gathered by Mazzoli *et al.*,[10] on the variation of secondary Stokes parameters with the primary polarization measured in Bragg diffraction at the Cr K pre-edge of potassium chromate (K_2CrO_4). By exploiting previously established knowledge of the crystal structure of the compound and formally exact expressions for scattering amplitudes, we fit the available data. An important point is that the small deviation of −0.783° from the origin of the azimuthal angle reported in Ref. 10 should be taken into account in order to justify the lack of symmetry of the curves at the point $\eta=0$. The model without an E2-E2 contribution gives an azimuthal dependence that is mainly due to the E1-E2 event intensity, with a small E1-E1 contribution, and that would most plausibly consider the pre-edge feature in the energy profile as being of the E1-E2 origin with a good degree of approximation. We have also explored the possibility of the existence of an E2-E2 contribution. If we allow the E2-E2 contribution, the fitting will show that the E2-E2 contribution will be dominant. If we use the parameters obtained in this fit to simulate the azimuthal dependence of the (140) and (340) reflections, we will obtain a good agreement with experimental data.[8] However, this finding seems to clash with the fact that an E2-E2 contribution should be absent or small, provided that the Cr^{6+} isolated ion has an empty $3d$ shell, forbidding tensors involved in the E2-E2 event, and their appearance would only be justified for covalency with the neighboring oxygens. We provide estimates for the atomic multipoles allowed by symmetry. These include polar multipoles that are not accessible in a dichroic signal since natural circular dichroism is forbidden. A prediction is made for the two models used (forbidding and allowing the E2-E2 contribution) for the azimuthal dependence of intensity at the space-group-forbidden (130) reflection. Testing the prediction in future experiments will shed light on the angular anisotropy in the Cr environment and will severely challenge our model calculation.

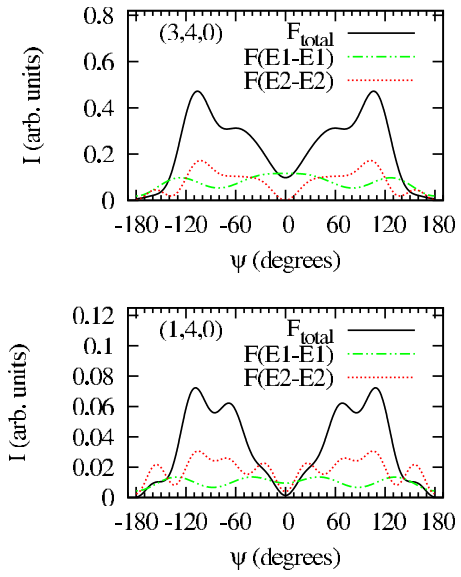

FIG. 9. (Color online) Azimuthal dependence of the intensity of the (140) and (340) reflections derived from the fitted parameters of the model with contributions from parity-even E2-E2 and E1-E1 channels. To obtain these curves, the fitted parameters in Eq. (11) were used. The primary linear polarization used is σ, and it is assumed that no polarizer is used for measuring the intensity of the secondary beam. We assume that at $\psi=0$, the c axis is initially parallel to the z axis in the x-ray coordinates (Ref. 1).

ACKNOWLEDGMENTS

Financial support has been received from Spanish MECD Grant No. MAT2005–06806–C04–01. One of us (J.F.-R.) is grateful to Gobierno del Principado de Asturias for the financial support from Plan de Ciencia, Tecnología e Innovación (PCTI) de Asturias 2006–2009. S.W.L. is grateful to Carsten Detlefs for discussions and correspondence on several aspects of the interpretation of x-ray experiments on K_2CrO_4. J.F.R. and J.A.B. acknowledge discussions with Claudio Mazzoli and François de Bergevin. P. J. Brown kindly scrutinized the crystal physics used in our analysis. Immediately prior to the submission of our paper for publication, we received from the authors of Ref. 10 a revised version of their work. In the revised preprint, an offset in the orientation of the crystal is specified, which is just what we find necessary in order to achieve a good analysis of data for secondary Stokes parameters.

APPENDIX A: EXPRESSIONS FOR THE INTENSITY AND SECONDARY STOKES PARAMETERS

Here, we present expressions of the intensity I_0 and Stokes parameters of the secondary polarization (P_1', P_2', P_3')

as functions of the primary beam Stokes parameters (P_1, P_2, P_3),. $G_{\mu\nu}$ are the total cross sections for the different polarization states,[1,12]

$$I_0 = \frac{1}{2}(1+P_3)(|G_{\sigma'\sigma}|^2 + |G_{\pi'\sigma}|^2) + \frac{1}{2}(1-P_3)(|G_{\pi'\pi}|^2 + |G_{\sigma'\pi}|^2) + P_2\,\mathrm{Im}(G^{\star}_{\sigma'\pi}G_{\sigma'\sigma} + G^{\star}_{\pi'\pi}G_{\pi'\sigma}) + P_1\,\mathrm{Re}(G^{\star}_{\sigma'\sigma}G_{\sigma'\pi} + G^{\star}_{\pi'\pi}G_{\pi'\sigma}), \quad \text{(A1)}$$

$$I_0P'_1 = (1+P_3)\mathrm{Re}(G^{\star}_{\sigma'\sigma}G_{\pi'\sigma}) + (1-P_3)\mathrm{Re}(G^{\star}_{\pi'\pi}G_{\sigma'\pi}) + P_2\,\mathrm{Im}(G^{\star}_{\sigma'\pi}G_{\pi'\sigma} + G^{\star}_{\pi'\pi}G_{\sigma'\sigma}) + P_1\,\mathrm{Re}(G^{\star}_{\pi'\pi}G_{\sigma'\sigma} + G^{\star}_{\sigma'\pi}G_{\pi'\sigma}), \quad \text{(A2)}$$

$$I_0P'_2 = (1+P_3)\mathrm{Im}(G^{\star}_{\sigma'\sigma}G_{\pi'\sigma}) - (1-P_3)\mathrm{Im}(G^{\star}_{\pi'\pi}G_{\sigma'\pi}) + P_2\,\mathrm{Re}(G^{\star}_{\sigma'\sigma}G_{\pi'\pi} - G^{\star}_{\pi'\sigma}G_{\sigma'\pi}) + P_1\,\mathrm{Im}(G^{\star}_{\sigma'\sigma}G_{\pi'\pi} - G^{\star}_{\pi'\sigma}G_{\sigma'\pi}), \quad \text{(A3)}$$

$$I_0P'_3 = \frac{1}{2}(1+P_3)(|G_{\sigma'\sigma}|^2 - |G_{\pi'\sigma}|^2) + \frac{1}{2}(1-P_3)(|G_{\sigma'\pi}|^2 - |G_{\pi'\pi}|^2) + P_2\,\mathrm{Im}(G^{\star}_{\sigma'\pi}G_{\sigma'\sigma} - G^{\star}_{\pi'\pi}G_{\pi'\sigma}) + P_1\,\mathrm{Re}(G^{\star}_{\sigma'\pi}G_{\sigma'\sigma} - G^{\star}_{\pi'\pi}G_{\pi'\sigma}). \quad \text{(A4)}$$

APPENDIX B: AMPLITUDES PRODUCED BY THE E1-E1, E2-E2, AND E1-E2 RESONANT EVENTS

For $(hk0)$ reflections, the calculated unit-cell structure factors for the different resonant events in the different polarization channels are obtained by substituting the dependence of Ψ_Q^K given by Eqs. (6) and (7) into Eq. (5). Analytical expressions are given by

$$F_{\sigma'\sigma}(\text{E1-E1}) = \Psi_1^{2,\text{E1-E1}}\sin 2\psi \sin\alpha, \quad \text{(B1)}$$

$$F_{\pi'\pi}(\text{E1-E1}) = \Psi_1^{2,\text{E1-E1}}\sin 2\psi \sin\alpha \sin^2\theta, \quad \text{(B2)}$$

$$F_{\pi'\sigma}(\text{E1-E1}) = \Psi_1^{2,\text{E1-E1}}(\cos 2\psi \sin\alpha \sin\theta - \cos\psi\cos\alpha\cos\theta), \quad \text{(B3)}$$

$$F_{\sigma'\sigma}(\text{E2-E2}) = \sin 2\psi\left\{\frac{1}{2}\sqrt{\frac{3}{7}}\Psi_1^{2,\text{E2-E2}}\sin\alpha\sin^2\theta + \frac{1}{2\sqrt{14}}\Psi_1^{4,\text{E2-E2}}\sin\alpha[2\sin^2\theta(7\cos^2\psi - 3) - 7\cos 2\psi] + \frac{1}{2\sqrt{2}}\Psi_3^{4,\text{E2-E2}}\sin 3\alpha(2\cos^2\theta\sin^2\psi - 1)\right\}, \quad \text{(B4)}$$

$$F_{\pi'\pi}(\text{E2-E2}) = \sin 2\psi\left\{\frac{1}{2}\sqrt{\frac{3}{7}}\Psi_1^{2,\text{E2-E2}}\sin\alpha\cos 4\theta + \frac{1}{4\sqrt{14}}\Psi_1^{4,\text{E2-E2}}\sin\alpha[2 + \sin^2 2\theta(3 - 7\cos^2\psi)] + \frac{1}{4\sqrt{2}}\Psi_3^{4,\text{E2-E2}}\sin 3\alpha(\sin^2 2\theta\sin^2\psi - 2)\right\}, \quad \text{(B5)}$$

$$F_{\pi'\sigma}(\text{E2-E2}) = \frac{1}{2}\sqrt{\frac{3}{7}}\Psi_1^{2,\text{E2-E2}}(-\cos 2\psi\sin\alpha\sin 3\theta + \cos\psi\cos\alpha\cos 3\theta) + \frac{1}{2\sqrt{14}}\Psi_1^{4,\text{E2-E2}}\{\cos\psi\cos\alpha(\cos 3\theta - 7\sin^2\psi\cos^3\theta) + \sin\alpha[-\sin 3\theta + \sin^2\psi\sin\theta(27 - 29\sin^2\theta - 28\sin^2\psi\cos^2\theta)]\} + \frac{1}{2\sqrt{2}}\Psi_3^{4,\text{E2-E2}}\{\cos\psi\cos 3\alpha\cos\theta(1 - 3\sin^2\psi\cos^2\theta) - \sin 3\alpha\sin\theta[1 - \sin^2\psi(5 - 3\sin^2\theta - 4\sin^2\psi\cos^2\theta)]\}, \quad \text{(B6)}$$

$$F_{\sigma'\sigma}(\text{E1-E2}) = \frac{1}{\sqrt{30}}\sin 2\psi\sin 2\alpha\sin\theta(-i2\sqrt{2}\Psi_2^{3,u} + \Psi_2^{2,u}), \quad \text{(B7)}$$

$$F_{\pi'\pi}(\text{E1-E2}) = -\frac{1}{\sqrt{30}}\sin 2\psi\sin 2\alpha(i2\sqrt{2}\Psi_2^{3,u}\sin^3\theta + \Psi_2^{2,u}\sin 3\theta), \quad \text{(B8)}$$

$$F_{\pi'\sigma}(\text{E1-E2}) = i\frac{\sqrt{3}}{10}\Psi_0^{1,u}\cos\psi\sin 2\theta - i\frac{1}{5\sqrt{2}}\Psi_0^{3,u}\cos\psi\sin 2\theta + i\frac{\Psi_2^{3,u}}{\sqrt{15}}(\cos\psi\cos 2\alpha\sin 2\theta - 2\cos 2\psi\sin 2\alpha\sin^2\theta)$$

$$+\frac{1}{\sqrt{30}}\Psi_2^{2,u}\{\sin 2\alpha[\sin\psi^2(3-5\sin^2\theta)-1-2\cos 2\theta]-2\cos\psi\cos 2\alpha\sin 2\theta\}, \quad \text{(B9)}$$

where $\theta = 32.8°$ is the Bragg angle of the (130) reflection. The structure factors in the $\sigma'\pi$ channel are readily obtained from structure factors in the $\pi'\sigma$ channel by using the relationships $F_{\sigma'\pi}(\theta) = F_{\pi'\sigma}(-\theta)$ for parity-even events and $F_{\sigma'\pi}(\theta) = -F_{\pi'\sigma}(-\theta)$ for parity-odd events. It is important to note that all calculated unit-cell structure factors $F_{\mu\nu}$ are purely real quantities.

[1] S. W. Lovesey, E. Balcar, K. S. Knight, and J. Fernández-Rodríguez, Phys. Rep. **411**, 233 (2005).

[2] Y. Tanaka, T. Inami, S. W. Lovesey, K. S. Knight, F. Yakhou, D. Mannix, J. Kokubun, M. Kanazawa, K. Ishida, S. Nanao, T. Nakamura, H. Yamauchi, H. Onodera, K. Ohoyama, and Y. Yamauchi, Phys. Rev. B **69**, 024417 (2004).

[3] D. F. McMorrow, K. A. McEwen, U. Steigenberger, H. M. Rønnow, and F. Yakhou, Phys. Rev. Lett. **87**, 057201 (2001).

[4] S. W. Lovesey, J. Fernández Rodríguez, J. A. Blanco, and P. J. Brown, Phys. Rev. B **70**, 172414 (2004).

[5] J. Fernández-Rodríguez, J. A. Blanco, P. J. Brown, K. Katsumata, A. Kikkawa, F. Iga, and S. Michimura, Phys. Rev. B **72**, 052407 (2005).

[6] S. W. Lovesey, J. Fernández-Rodríguez, J. A. Blanco, D. S. Sivia, K. S. Knight, and L. Paolasini, Phys. Rev. B **75**, 014409 (2007).

[7] S. W. Lovesey, J. Fernández-Rodríguez, J. A. Blanco, and Y. Tanaka, Phys. Rev. B **75**, 054401 (2007).

[8] D. H. Templeton and L. K. Templeton, Phys. Rev. B **49**, 14850 (1994).

[9] C. Theil, J. van Elp, and F. Folkmann, Phys. Rev. B **59**, 7931 (1999).

[10] C. Mazzoli, S. B. Wilkins, S. Di Matteo, B. Detlefs, C. Detlefs, V. Scagnoli, L. Paolasini, and P. Ghigna, Phys. Rev. B **76**, 195118 (2007).

[11] L. Paolasini *et al.*, J. Synchrotron Radiat. **14**, 301 (2007).

[12] S. Lovesey and S. Collins, *X-Ray Scattering and Absorption by Magnetic Materials* (Clarendon, Oxford, 1996).

[13] L. Landau and E. Lifshitz, *Electrodynamics of Continuous Media* (Pergamon, Oxford, 1982).